Simulating entangled sources by classically correlated sources and quantum imaging

Morton H. Rubin
Department of Physics
University of Maryland, Baltimore County
Baltimore, MD 21228-5398
(February 1, 2008)

We discuss the problem of when a set of measurements made on an entangled source can be simulated with a classically correlated source. This is discussed in general and some examples are given. The question of which aspects of quantum imaging can be simulated by classically correlated sources is examined.

03.65.Ud,42.50.Dv,42.30.Va

arXiv:quant-ph/0303188v2 29 Jul 2003

I. INTRODUCTION

Recently there has been a discussion in the literature about when an imaging experiment carried out with spontaneous parametric down conversion (SPDC) can be simulated classically [1,2]. We wish to discuss this problem in the general setting of quantum information theory and to give a class of experiments in which the measurements with a given entangled source can be reproduced using a classically correlated source. In addition, we show that certain aspects of the "ghost" interference experiment [3] can be reproduced using a classically correlated source. It is very important to have a clear understanding of what is being simulated. We show that while certain results can be reproduced by classically correlated sources, those results that depend on the phase of the two photon amplitude or biphoton can not. For a review of quantum imaging see ref. [4,5].

There has been a great deal of work done on determining whether a given state is entangled. The problem discussed here is different, we ask when the results of the experiment using a source that produces an entangled state can be reproduced by replacing the entangled state by a separable state. In the imaging experiments an entangled initial state is generated by SPDC and is transformed into the output state by the fields propagating through a linear optical system. The most important point is that the system has loss in it, indeed, the image is formed by removing photons from one of the beams. Loss may transform the state from an entangled state to a classically correlated state. When this happens all the measurements can be reproduced by a classically correlated source. However, this is not the general case since, even after losses, the state may remain entangled. Consequently, only certain measurements may be reproduced classically. This is the case we wish to discuss in this paper. The problem of substituting a stochastic classical source for a quantum source in optics experiments has been discussed many times. In the context of this paper, two reviews by Belinskii and Klyshko [6] are of interest.

It is important to be clear what we mean by an experiment. The original imaging experiment using SPDC [7] consisted of a source of entangled photon pairs with each photon passing through a linear optical system to detectors. A measurement consisted of the coincident detection of the pair. Each photon was detected locally and the coincidence triggering corresponded to classical communication. The outcome was summed over many such pairs. In the original experiment one detector scanned the image plane but this can be eliminated by placing a CCD detector in the image plane. In this case the experiment is series of measurements performed on a fixed setup that measures the intensity correlation function $\langle I_A(\mathbf{r}_1)I_B(\mathbf{r}_{2j})\rangle$ where the I 's are the normally ordered intensities and $j = 1, \cdots, N$ indexes the detectors in the CCD array. Note that these are N commuting operators. In the experiment of Bennink, *et. al.* [1] the source is replaced by a laser, beam splitters, a chopper and a moving mirror. In this case each measurement corresponds to a point by point scanning of the object plane. Light detected behind the object triggers the image plane detectors to their *on state* and the detector corresponding to the image point responds. The two experiments are related by replacing the SPDC source by a classical source. The classical source is meant to simulate a stochastic source that has a large bandwidth in the transverse wave numbers. If this bandwidth is the same as the bandwidth for SPDC, there will be no image behind the object plane.

These experiments should be contrasted with a test of a Bell inequality [8]. Such a test consists of a series of experiments for which the source is fixed but the measurement operators are different. This is important because the quantities measured at *each* site are non-commuting operators, so they can not be measured simultaneously. It has been recognized for a long time that any experiment which only measures a fixed set of local operators can be reproduced by a local hidden variable theory in which the probabilities for each outcome of the experiment are themselves taken as the local variables. Then any correlations that exist can be modelled by separable density matrices, a simple example is given in section III. The experimental results of [1] are consistent with this conclusion. Some

SPDC experiments can be understood in terms of a picture first proposed by Klyshko [9,10] in which one detector is viewed as a source of photons propagating backwards in time, reflecting off the SPDC crystal, and then propagating forward in time to the second detector. It is often not appreciated that this picture has a rigorous mathematical foundation for maximally entangled photon pairs. This picture is genralized in VI C so it can be used to explain the experiment similar to that in ref. [1]. However, as can be seen, results that depend on fixed phase relations between two-photon amplitudes can not be simulated. Furthermore, it should be remembered that the quantum or classical nature of a state is determined by the statistics of the experiment, so even if the average of a set of measurements can be reproduced classically, it does not follow that the fluctuations in correlation measurements can be reproduced by classically correlated systems. In the imaging experiment there are two important results such that, as we shall see below, one can be simulated but the other can not. For a different perspective on this problem see ref. [11].

In the following we will analyze the statements made above and give examples of when an experiment using an entangled input state can be simulated by a classically correlated input state. We first review some well-known results about measurements and entanglement, and apply them to the simple case of two qubits to illustrate some of the issues discussed above. Then we discuss the imaging experiments.

II. BACKGROUND

For all the experiments that we discuss assume that the source produces a pair of subsystems A and B in a state ρ_{AB}. The subsystems are sent to two separate sites, also denoted by A and B, where local measurements are made. The Hilbert space describing the system is $H = H_A \otimes H_B$. The set of observables is defined by $\{O_{AB}^{(i,j)} = O_A^{(i)} \otimes O_B^{(j)} \quad (i,j) \in S\}$ acting on H where the sets of Hermitian operators $\{O_A^{(i)}\}$ and $\{O_B^{(j)}\}$ act on H_A and H_B, respectively. A state σ_{AB} is said to be separable or classically correlated if it can be written in the form

$$\sigma_{AB} = \sum_u p_u \sigma_A^{(u)} \otimes \sigma_B^{(u)} \tag{1}$$

where $\{p_u\}$ is a probability distribution, *i.e.* a set of positive numbers that sums to 1, and σ_A (σ_B) is a density matrix acting on H_A (H_B). An experiment will be defined to be classical (more precisely, classically correlated) if there exists a separable state such that for all $(i,j) \in S$

$$tr O_{AB}^{(i,j)} \rho_{AB} = tr O_{AB}^{(i,j)} \sigma_{AB} \tag{2}$$

We may actually be content to simulate one observable that is a linear combination of direct product observables,

$$O_{AB} = \sum_{ij} q_{ij} O_{AB}^{(i,j)}. \tag{3}$$

All of these are correlation experiments for which the experimentalists agree which pair of observables they measure for a given realization of the experiment. For example if the polarization of a pair of photons is measured then $i = H$ or V corresponding to the measurement of a horizontal or vertical polarization in A, and similarly for the measurement in B, $j = H$ or V. The four possible projection operators are not only pairwise commuting but are locally pairwise commuting, consequently, the experiment can be performed using one fixed set-up in each laboratory. On the other hand if, for example, $i = H, V, R$ and L where R and L refer to right and left hand polarized light, then the observables in A do not all commute and can not be measured simultaneously[1]. There may be more than one classically correlated state that can simulate a given experiment. If this is the case, the set of such states will form a convex set [12]. A simple illustrative example for qubits is given in section III where these measurements are discussed in a geometrical context.

We illustrate how an experiment on an entangled state can be simulated using a separable state by a simple example. Consider an entangled pure state Ψ, let $O_{AB} = O_A \otimes O_B$ be an observable, and let $\{\phi_j\}$ be the set of eigenvectors of O_A. Let $\{\chi_j\}$ be an orthonormal basis of H_B and consider the arbitrary state

[1]Of course it is possible to use a beam splitter to send half the photons to the pair of detectors that measures H and V and the other half to detectors that measure R and L but this does not change the argument.

$$\Psi = \sum_{j,k=1}^{N} c_{jk}\phi_j \otimes \chi_k. \tag{4}$$

The measurement of O_{AB} gives

$$tr\left(O_{AB}|\Psi\rangle\langle\Psi|\right) = \sum_j \lambda_j \langle\chi_j|O_B|\chi_j\rangle |c_j|^2 \tag{5}$$

where $O_A\phi_i = \lambda_i\phi_i$. It is not difficult to see that we get the same result for the classically correlated state

$$\sigma = \sum_j |\phi_j\rangle\langle\phi_j| \otimes |\omega_j\rangle\langle\omega_j| \quad |\omega_j\rangle = \sum_k c_{jk}|\chi_k\rangle. \tag{6}$$

Therefore, any simple local measurement, that is, a measurement of a direct product of local operators, can be simulated by a separable measurement.

Now consider a different observable obtained by a unitary transformation applied to O_A, $O'_{AB} = O'_A \otimes O_B$, such that $O'_A = U^\dagger O_A U$ and O_A do not commute. For example if subsystem A is a spin-1/2 particle and $O_A = \sigma_z$ take $O'_A = \sigma_x$. It is not difficult to show that the new measurements are not produced by the same classically correlated state since $\langle\phi_k|O'_A|\phi_j\rangle \neq \lambda_j\delta_{kj}$ in general. Finally if $\{O_{AB}^{(i,j)},\ i,j \in S\}$ where the $\{O_A^{(i)}\}$ are pairwise commuting operators, this result immediately generalizes since the $\{\phi_j\}$ can be taken as simultaneous eigenvectors of all the $O_A^{(i)}$.

It is worth noting that if $trO_{AB} = 0$ we can always find a separable state $\sigma(s_0)$ such that $trO_{AB}\rho = (1/s_0)trO_{AB}\sigma(s_0)$. To see this let ρ be the given entangled state on an N dimensional Hilbert space, I_N the identity operator, and D_0 be the completely random state, $D_0 = (1/N)I_N$ [13]. The convex combination $\sigma(s) = (1-s)D_0 + s\rho$ is a state of the system which is entangled for $s = 1$ and classically correlated for $s = 0$. Therefore, there exists an $s_0 \in (0,1)$ such that the state $\sigma(s) = (1-s)D_0 + s\rho$ is classically correlated for $s \leq s_0$ [14]. The reason for mentioning this is that many experiments do not look at absolute values but at relative values for which the normalization of the density matrices is not important.

In a typical experiment, the state of the system measured, ρ_{AB}, is related to an input state, ρ_{0AB}, by a completely positive, trace preserving, linear transformation

$$\rho_{AB} = T(\rho_{0AB}). \tag{7}$$

The Kraus representation of T [15,16] is

$$\rho_{AB} = T(\rho_{0AB}) = \sum_{k=1}^{n} V_k \rho_{0AB} V_k^\dagger \tag{8}$$

where the set of operators $\{V_k, k = 1, \cdots, n\}$ acting on H satisfy

$$\sum_{k=1}^{n} V_k^\dagger V_k = I_H \tag{9}$$

with I_H is the identity operator on H. In the experiments of interest in this paper, each of the operators V_k is a direct product of operators acting on H_A and H_B,

$$V_k = A_k \otimes B_k, \tag{10}$$

In quantum optics experiments the V_k can be computed from classical optics. Using eq. (8) we have

$$\begin{aligned} trO_{AB}\rho_{AB} &= \sum_{k=1}^{n} trO_{AB}\left(V_k\rho_{0AB}V_k^\dagger\right) \\ &= \sum_{k=1}^{n} tr\left(V_k^\dagger O_{AB} V_k\right)\rho_{0AB} \end{aligned} \tag{11}$$

the first line is referred to as the Schrödinger picture and the second line as the Heisenberg picture. Using our locality assumptions

$$V_k^\dagger O_{AB} V_k = A_{k_1}^\dagger O_A A_{k_1} \otimes B_{k_2}^\dagger O_B B_{k_2} \quad k = (k_1, k_2). \tag{12}$$

We can now rewrite eq. (2) as

$$tr O_{AB}^{(i,j)} \rho_{AB} = \sum_u p_u \left(tr O_A^{(i)} \sigma_A^{(u)} \right) \left(tr O_B^{(j)} \sigma_B^{(u)} \right). \tag{13}$$

If both $O_A^{(i)}$ and $O_B^{(j)}$ are positive operators then the right hand side of eq. (13) is the sum of positive terms and there can be no relative phase information about the subsystems extracted from this expression. Then since any Hermitian operator can be written as a difference of two positive operators, there is a stringent condition on the type of experiment that can be simulate by classically correlated systems.

It will be useful to record a few well-known results for pure states. Let Ψ be a pure state with Schmidt representation given by

$$\Psi = \sum_{k=1}^{N} c_k |\phi_k\rangle \otimes |\chi_k\rangle \tag{14}$$

[16]. Recall that the set $\{|c_k|^2, k = 1, \cdots, N\}$ is a probability distribution and the states $\{\phi_k\}$ and $\{\chi_k\}$ are orthonormal sets in H_A and H_B, respectively. The state Ψ is separable if $c_k = \delta_{k1}$, otherwise it is entangled. If $c_k = 1/\sqrt{N}$, the state is said to be maximally entangled. For a maximally entangled pure state $\Psi^{(M)}$ a Kraus operator applied at one subsystem can be replaced by an operator applied at the second subsystem,

$$\left(A_s \otimes B_r\right) \Psi^{(M)} = \left(1_A \otimes B_r A_s^T\right) \Psi^{(M)}, \tag{15}$$

where $A_s \phi_j = \sum_k \phi_k \left(A_s\right)_{kj}$ and $A_s^T \chi_k = \sum_j \chi_j \left(A_s\right)_{kj}$. In experiments it is often useful to place objects corresponding to Kraus operators such as beam splitters or lenses in both laboratories A and B, however, for maximally entangled states this is entirely equivalent putting them all in one of the laboratories. This fact is exploited in remote state preparation [17–19].

III. ENTANGLEMENT WITNESSES

For finite dimensional systems the question of whether a given state, represented by an $N \times N$ density matrix, is entangled can be answered by operators, called entanglement witnesses [20,21], in the space of Hermitian operators. Entanglement witnesses have a geometric interpretation as hyperplanes that separate a given entangled state from the separable states [20–22]. In this geometric picture, an optimal entanglement witness is one which is tangent to the surface of the separable states. Recently, the optimal entanglement witnesses have been characterized in terms of a set of coordinated local measurements [23,24]. An entanglement witness, W, is defined for an entangled state ρ as a Hermitian operator such that

$$tr(\rho W) < 0, \tag{16}$$

and for any separable density matrix τ

$$tr(\tau W) \geq 0. \tag{17}$$

The entanglement witness is said to be optimal if there exists a separable density τ_0 such that equality holds, that is, W determines a plane tangent to the separable states.

Consider the simplest case of two qubits [23,24]. We shall denote the Pauli matrices by σ_μ, $\mu = 0, \cdots, 3$ where σ_0 is the 2×2 identity matrix. Consider the state

$$\rho = |\Phi_+\rangle\langle\Phi_+| \tag{18}$$

where $\Phi_+ = \frac{1}{\sqrt{2}} \left(|00\rangle + |11\rangle\right)$ is one of the Bell states, $|0\rangle$ corresponds to the spin-up state, and $|1\rangle$ the spin-down state in the basis in which the Pauli matrix σ_3 is diagonal. It has been shown that the optimal entanglement witness for this state is

$$W = \frac{2}{3} \left(\sigma_0 \otimes \sigma_0 - 3\tau_0\right) \tag{19}$$

where τ_0 can be written in terms of local projection operators, the factor of 2/3 is a normalization. For $j = 1, 2, 3$ define the projections

$$P_j^{\pm} = \frac{1}{2}\left(\sigma_0 \pm \sigma_j\right) \tag{20}$$

and

$$P_j^{ab} = P_j^a \otimes P_j^b, \tag{21}$$

then

$$\tau_0 = \frac{1}{6}\left[\left(P_3^{++} + P_3^{--}\right) + \left(P_1^{++} + P_1^{--}\right) + \left(P_2^{+-} + P_2^{-+}\right)\right]. \tag{22a}$$

We see that τ_0 can be written as the sum of three pairwise commuting operators that are, however, locally non-commuting observables corresponding to the measurement each spin along one of three orthogonal axes. For a fixed experimental set-up, one of the pairs of operators in the parentheses can be measured. For example, the measurement of the state in eq. (18) along the 1-axis can be reproduced using the separable state

$$\tau = P_1^{++}\rho P_1^{++} + P_1^{--}\rho P_1^{--} = \frac{1}{2}\left(P_1^{+} \otimes P_1^{+} + P_1^{-} \otimes P_1^{-}\right). \tag{23}$$

Similarly, the other two measurements can be reproduced if the input state is a (different) separable state. However the measurement $trW\rho < 0$ can not be reproduced by a separable state, τ, since for all such state $trW\tau \geq 0$.

We can exploit this geometric picture further to show that there may be many observables that will satisfy eq. (13). Let τ_0 be the nearest separable state to ρ in the sense that

$$||\rho - \tau|| = \sqrt{tr\left[(\rho - \tau)^2\right]} \geq ||\rho - \tau_0|| \tag{24}$$

for all separable states τ. Then there is an optimal entanglement witness for ρ through τ_0. Suppose τ_0 has rank greater than one. Then the hyperplane of the entanglement witness intersects the separable densities in, at least, a line containing τ_0. For any separable state τ on the line

$$tr\left[(\rho - \tau_0)(\tau - \tau_0)\right] = 0. \tag{25}$$

Using the fact that the separable density matrices form a compact convex set, we can write

$$\tau - \tau_0 = \sum_u a_u \sigma_A^{(u)} \otimes \sigma_B^{(u)} \tag{26}$$

where the a_u are real but not necessarily positive and the $\sigma_A^{(u)} \otimes \sigma_B^{(u)}$ are extreme points of the line. Therefore, $\tau - \tau_0$ is an observable that corresponds to local measurements with classical communications, consequently, when the system is in the entangled state ρ its measurement of this variable can be simulated using the separable state τ_0.

IV. SPDC EXPERIMENTS

The general theory of the type of experiment shown in fig. 1 has been given in [25]. The source discussed in that paper was maximally entangled in frequency and transverse wave number. It was pointed out that the source ρ_0 could be envisioned as entangled in transverse modes which are not necessarily plane wave modes. In the present context these modes are generated by the POVM's acting on the maximally entangled transverse modes of the beams generated by the SPDC crystal. Specifically, suppose the pump is a plane wave of angular frequency ω_p normally incident on a crystal that is infinite in the transverse direction. The state of the down converted biphoton is

$$\Psi_0 = \sum_j f_j a_s^{\dagger}(\omega_j, \mathbf{p}_j) a_i^{\dagger}(\omega_p - \omega_j, -\mathbf{p}_j)|0\rangle \tag{27}$$

where $a_r^{\dagger}(\omega, \mathbf{p})$ is the creation operator for a photon at the output face of the crystal with polarization r, frequency ω, and transverse wave vector $\mathbf{p}$. Then we can write the state propagated to the detectors located at $\mathbf{r}_1$ and $\mathbf{r}_2$

$$\Psi_{AB} = \sum_j g_A(\mathbf{r}_1, \omega_j, \mathbf{p}_j) g_B(\mathbf{r}_2, \omega_p - \omega_j, -\mathbf{p}_j) f_j a_s^\dagger(\omega_j, \mathbf{p}_j) a_i^\dagger(\omega_p - \omega_j, -\mathbf{p}_j)|0\rangle$$
$$= \sum_j f_j a_s^\dagger(\mathbf{r}_1, \omega_j, \mathbf{p}_j) a_i^\dagger(\mathbf{r}_2, \omega_p - \omega_j, -\mathbf{p}_j)|0\rangle \tag{28}$$

where the operators in second line are defined in the obvious way (cf. eq. (12)). For example,

$$a_s^\dagger(\mathbf{r}_1, \omega_j, \mathbf{p}_j) = g_A(\mathbf{r}_1, \omega_j, \mathbf{p}_j) a_s^\dagger(\omega_j, \mathbf{p}_j). \tag{29}$$

is the creation operator at detector one. The propagators g are determined by the linear optical systems in each arm of the experiment (see appendix VI A and [25] for detailed calculations). They can be expanded in terms of any convenient set of orthogonal transverse modes as is usually done when the field propagates in a fiber. It may be useful to recall that $g_A(\mathbf{r}_1, \omega_j, \mathbf{p}_j)$ is a transformation from the transverse momentum $\mathbf{p}_j$ to the transverse position $\mathbf{r}_{1T}$. The mode label j and the longitudinal variable $\mathbf{r}_{1L}$ are parameters

It is the entanglement of the pair in their transverse coordinates that is most important for image transfer. In many experiments the maximally entangled state is a good approximation. As shown in eq. (15), it is the maximal entanglement that makes it possible to put all the optics in one arm. If the pump is not a plane wave Ψ_0 is no longer maximally entangled in the transverse direction.

In the quantum imaging papers using SPDC one produces an image or interference pattern in coincident counting. Since the SPDC has a large wave number bandwidth even for a narrow frequency range there is no image or interference pattern behind the object plane. Both of these effects can be simulated by classically correlated sources. A second important feature of the quantum case is the relation between the position of the aperture in one arm and the detector array in the second arm. These relations depend on the phase relation between the two-photon amplitudes or biphoton and, as we shall see, can not be reproduced by classically correlated sources. This is a specific example of the result discussed in connection with eq. (13).

Starting with eq. (28) we can first ask what happens if we simply detect all the photons at B discarding all the photons at A

$$\rho_B = tr_A |\Psi_{AB}\rangle\langle\Psi_{AB}|$$
$$= \sum_{jk} f_{jk} a_i^\dagger(\mathbf{r}_2, \omega_p - \omega_j, -\mathbf{p}_j)|0\rangle\langle 0| a_i(\mathbf{r}_2, \omega_p - \omega_k, -\mathbf{p}_k) \tag{30}$$

where

$$f_{jk} = f_j f_k^* \int d^2\mathbf{r}_{1T}\ g_A(\mathbf{r}_1, \omega_j, \mathbf{p}_j) g_A^*(\mathbf{r}_1, \omega_k, \mathbf{p}_k) \tag{31}$$

and $\mathbf{r}_{1T}$ is the transverse component of $\mathbf{r}_1$. As pointed out in [1,2], if g_A is unitary the $f_{ik} = |f_j|^2 \delta_{ik}$ and the marginal density is the same as that of the source. We have not put indices on the g_A and g_B because we are concerned with a fixed experimental set-up. However, if we consider different set-ups, as we would in testing Bell inequalities, then we need to index them.

We now consider coincidence detection. For simplicity we take our detectors to be polarization independent, point detectors oriented along the $\widehat{\mathbf{e}}_L$ direction. The electric field operator for such a detector located at $\mathbf{r}$ is given by

$$E = E^{(+)} + E^{(-)} \quad E^{(-)} = E^{(+)\dagger}$$
$$E^{(+)}(\mathbf{r}, t) = \sum_{j,q} E_j a_q(\omega_j, \mathbf{p}_j) e^{i(\mathbf{k}_j \cdot \mathbf{r} - \omega t)} \quad \mathbf{k}_j = \mathbf{p}_j + \widehat{\mathbf{e}}_L \sqrt{\frac{\omega_j^2}{c^2} - p_j^2} \tag{32}$$

where E_j is determined by dimensional considerations, q is the polarization index, and $p_j << \omega/c$. The probability of two detectors firing is proportional to

$$tr\left(\rho_{AB} E_2^{(-)} E_1^{(-)} E_1^{(+)} E_2^{(+)}\right) = |A_{12}|^2 \tag{33}$$

where

$$A_{12} = \langle 0| E_1^{(+)} E_2^{(+)} |\Psi_{AB}\rangle = \langle 0| E^{(+)}(\mathbf{r}_1, t_1) E^{(+)}(\mathbf{r}_2, t_2)|\Psi_{AB}\rangle$$
$$= \sum_j g_A(\mathbf{r}_1, \omega_j, \mathbf{p}_j) g_B(\mathbf{r}_2, \omega_p - \omega_j, -\mathbf{p}_j) f_j E_j E_h e^{-i\omega_j t_1 \pi} e^{-i\omega_h t_2}, \tag{34}$$

$\omega_h = \omega_p - \omega_j$, and $\mathbf{k}_h = -\mathbf{p}_j + \widehat{\mathbf{e}}_L\sqrt{\frac{\omega_j^2}{c^2} - p_j^2}$. A_{12} is the biphoton amplitude.

In the imaging experiments one detector collects all the light that passes through the object, T in fig. 1, *i.e.* the correlation that is measured is the correlation when the transverse component of $\mathbf{r}_1$ is integrated over. To carry out the computation we assume degenerate phase matching so that we can write $\omega_1 = \omega_p/2 + \nu$ and $\omega_2 = \omega_p/2 + \nu'$ where frequency phase matching gives $\nu' = -\nu$. We require $|\nu| << \omega_p/2$. In the paraxial approximation we can write

$$A_{12} = \int d\nu u(\nu) e^{i\nu(t_1 - t_2)} e^{i\omega_P(t_1+t_2)/2} \frac{1}{K^2} \int d^2x t(\mathbf{x}) e^{-iK^2(\mathbf{x}_2 - \mathbf{x})^2} \tag{35}$$

where $t(\mathbf{x})$ is the transmission function of T, and

$$K = \left(\frac{2c}{\omega_p}\right)^2 \left(\frac{1}{d_1 + d_2} + \frac{1}{d_1'} - \frac{1}{F}\right). \tag{36}$$

The term containing K comes from converting the sum over j into an integral in the amplitude A_{12}, and is therefore an effect of the entanglement of the photons. When $K \to 0$, the Gaussian becomes a delta function and the coincident counting rate becomes proportional to $|t(\mathbf{x}_2)|^2$. The fact that the image and object planes are related by the geometrical optics condition $K = 0$ was derived and experimentally studied in [10] where it was also generalized to the case of non-degenerate SPDC.

We now ask whether this experiment can be simulated using a classically correlated source of coherent states. Consider the classically correlated state

$$\tau_{AB} = \sum_j q_j \tau_{AB}^{(j)}. \tag{37}$$

where $\{q_j,\, j = 1, 2, \cdots\}$ is a probability distribution,

$$\tau_{AB}^{(j)} = \tau_A^{(j)} \otimes \tau_B^{(j)} \quad \tau_X^{(j)} = |\psi_X^{(j)}\rangle\langle\psi_X^{(j)}| \quad X = A, B \tag{38}$$

and

$$\begin{aligned} |\psi_A^{(j)}\rangle &= \sum_m c_m^{(j)} |\{\alpha_m\}\rangle \\ |\psi_B^{(j)}\rangle &= \sum_m d_m^{(j)} |\{\beta_m\}\rangle \end{aligned} \tag{39}$$

The state $|\alpha_m\rangle$ is a coherent state generated by the creation operator $a_s^\dagger(\omega_m, \mathbf{p}_m)$ defined in eq. (27) and the coherent states $|\beta_m\rangle$ are generated by operators $a_i^\dagger(\omega_p - \omega_m, -\mathbf{p}_m)$. The restriction to coherent states is not strictly necessary to show that the results can be obtained from a classically correlated state, that is, we do not have to assume that the states sent to A and B are themselves "classical".

For the experiment illustrated in fig. 2, it is not difficult to show that

$$\begin{aligned} C &= \lim_{T\to\infty} \frac{1}{T} \int_0^T dt_1 \int_0^T dt_2 tr\left(\tau_{AB} E_2^{(-)} E_1^{(-)} E_1^{(+)} E_2^{(+)}\right) = \sum_j q_j tr_A\left(\tau_A^{(j)} E_1^{(-)} E_1^{(+)}\right) tr_B\left(\tau_A^{(j)} E_2^{(-)} E_2^{(+)}\right) \\ &= \int d^2p \int d^2p' q(\mathbf{p},\mathbf{p}') |g_A(\mathbf{r}_1, \omega_p/2, \mathbf{p})|^2 |g_B(\mathbf{r}_2, \omega_p/2, \mathbf{p}')|^2 \end{aligned} \tag{40}$$

[1,2], where we have converted the discrete sum over modes to integrals and defined

$$\sum_j q_j |c_m^{(j)}|^2 |d_{m'}^{(j)}|^2 |\alpha_m|^2 |\beta_{m'}|^2 \to d^2p d^2p' q(\mathbf{p},\mathbf{p}'). \tag{41}$$

Equation (40) is a special case of eq. (13) and contains no relative phase information between A and B. In arm B, the detector is placed in the focal plane of the second lens then, as shown in the appendix eq. (61), in the diffraction limited case

$$|g_B(\mathbf{r}_2, \omega_p/2, \mathbf{p}')|^2 = G\delta^{(2)}(\mathbf{p}' - \frac{\omega_p}{2c}\frac{1}{f_2}\mathbf{x}_2) \tag{42}$$

where $\mathbf{x}_2$ is the transverse coordinate of one of the point detectors located at D2. Taking the correlation function

$$q(\mathbf{p}, \mathbf{p}') = \delta^{(2)}(\varepsilon\mathbf{p}' - \mathbf{p}) \tag{43}$$

we get for the average number of coincident counts per pulse

$$C = C_0|t(\varepsilon\frac{f_1}{f_2}\mathbf{x}_2)|^2. \tag{44}$$

Note the detector in arm B and the object T are both in the focal plane of the lens. This can be interpreted as a point by point mapping of the mask onto the plane of the detectors at B. Equation (40) can be viewed as incoherent imaging [1,26]. The fact that a point by point imaging is at the heart of this type of experiment was noted some time ago in ref. [10].

The classically correlated source modelled here is a stochastic source that is broadband in spatial frequencies. This condition is included to ensure that there is no image in the $D1$ plane, as can be seen by setting $g_B = 1$ in eq. (40). The main characteristic of this source is that whenever it emits a beam to A with transverse wave number $\mathbf{p}$ it emits a beam to B with wave number $\mathbf{p}/\varepsilon$. The SPDC source has the same type of correlation but is significantly different because it imprints relative phase information on the beams in A and B which influences the correlation measurements. The important phase information exists in the transverse momentum dependent factors $\psi(\mathbf{p}, X)$ in eq. (49) and eq. (50). These phase factors disappear in eq. (40). This places stricter conditions on where the images are located than in SPDC.

The "ghost" interference experiment in ref. [3] displayed remarkable features. A simplified diagram is shown if fig. 3. The first important feature is that an interference pattern can be seen in the coincidence counting but if single photons are detected in the plane of $D1$ no interference is seen because the SPDC is a broad band spatial frequency source. The second feature is that the period of the interference pattern is determined by the distance z from T back to the surface of the crystal and then to $D2$. For the two slit experiment the coincident counting rate was proportional to $\cos^2(pd/2)$ where d is the slit separation and $p = 2\pi(x_2/z\lambda)$, x_2 being the position of a detector in array $D2$. A similar result holds for the single slit case. As the authors of ref. [3] point out: "The interference pattern is the same as one would observe on a screen in the lane of $D2$, if $D1$ is replaced by a point-like light source and the SPDC crystal by a reflecting mirror." This is just the Klyshko picture [9].

Let us examine this in a bit more detail. The detector $D1$ is at the origin of the plane at "infinity" so it detects the $\mathbf{p} = \mathbf{0}$ transverse mode. Since the SPDC is a broad band spatial source there are many different modes impinging on the slits. When a photon is detected by one of the detectors in $D2$ one of these modes $\mathbf{p}'$ is selected and we get coincidences when $p' \approx 2\pi n/d$ where d is the distance between the slits and n is an integer. For a given $\mathbf{p}'$ the maximum of the interference pattern in the plane at $D1$ corresponds to $\theta \approx p'/(\omega/c)$. Because of the broad bandwidth in p', this interference pattern is averaged over and is not visible without the coincidence measurement.

The interference pattern observed in [3] can also be simulated using a similar classically correlated source as is shown in VI B. As for the case discussed in [1], not all the features can be reproduced and the placement of the lenses $L1$ and $L2$ in fig. 2 play a critical role. It is important to understand what about these experiments is being simulated. In both cases the pattern, image or interference fringes, and the fact that there is no image or interference if one looks behind the object are simulated. The results relating the placement of detector $D2$ and the object T can not be simulated because, as we saw above, because this arises from phase information stored in the entangled system and not separately in the subsystems A and B. As in the imaging case this phase information is that in the factors $\psi(\mathbf{p}, X)$ in eq. (51) and eq. (52). From eq. (62) it is easy to see that for the double slit experiment the fringes are determined by $p = 2\pi(x_2/f_2\lambda)$, that is the distance z in the SPDC experiment has been replaced by the focal length of the lens in arm B.

In a recent paper [27] it has been shown that for an entangled source one can obtain both the image and its Fourier transform by only varying the position of a lens and the detector in the arm of the experiment that does not contain the aperture plane. This paper exploits the fact that for maximally entangled states one can locate the optics in either arm of the experiment. The authors explain their results by using entanglement, path indistinguishability, and complementarity in the transverse momentum and position. The complementarity argument must be made with care since it means different things to different people. The spatial and momentum (wave number) complementarity is a wave property and classical electromagnetic fields are waves. After all, one can display the spatial position and spatial frequencies of a source by simply changing the position of a lens. The path indistinguishability along with the quantum rule about adding amplitudes is more convincing since that invokes the particle properties of the photon which distinguish the quantum and classical pictures of the electromagnetic field. By using special cases of mixed state, the authors obtain a special case of eq. (13) and reach the same conclusions as those in this paper for the imaging case. However, they conclude, for their mixed states that they can not reproduce the interference fringes. This is not a general result, as we have shown.

We have shown that it is often possible to simulate some features of an experiment using an entangled source by a classically correlated source. Therefore, it is important when invoking entanglement as critical to an experimental result that the possibility of such a simulation is eliminated. Violation of Bell inequalities is a special case of using entanglement witnesses as observables to show that entanglement is necessary to explain some experimental measurements. Some quantum imaging experiments with SPDC sources are examples in which it is possible to simulate some of the measurements with classically correlated sources. In particular, the imaging pattern can be reproduced in coincidence counting even when there is no image or interference pattern visible behind the object. On the other hand, it is impossible to reproduce the aspects of the quantum experiments that depend on the relative phase information in the state of the entangled subsystems. This is a consequence of eq. (13).

We have not answered the general question of what local observables can be simulated by a classically correlated source for a given entangled source. Finally, it should be noted that the converse problem of when a classically correlated state can be used to study entanglement has been studied extensively starting with ref. [29].

V. ACKNOWLEDGMENTS

This work was stimulated by a NASA-DoD workshop held a JPL in November 2002 organized by Jonathan Dowling. I wish to express my gratitude for helpful comments from by colleagues at UMBC, particularly, Arthur O. Pittenger for comments and suggestions with regard to sections II and III, and to Milena D'Angelo and Yanhua Shih for discussions about the quantum imaging problem. This work was supported in part by NSF.

VI. APPENDIX

A. Notation

We briefly review the general form of a coincidence counting experiment [25]. The positive frequency part of the electric field at time t at the input of a detector located at $\mathbf{r} = z\widehat{\mathbf{e}}_z + \mathbf{x}$ is given by

$$E_\beta^{(+)}(\mathbf{r},t) = \int\int d\omega d^2p e^{-i\omega t} E(\omega) g\left(\mathbf{r},\omega,\mathbf{p}\right) a_\beta\left(\omega,\mathbf{p}\right),$$

where $a_\beta\left(\omega,\mathbf{p}\right)$ is the annihilation operator at the source for a photon of angular frequency ω, transverse wave number $\mathbf{p}$, and polarization β. The unit vector $\widehat{\mathbf{e}}_z$ is the inward normal to the surface of the detector, and $\mathbf{x}$ is the transverse coordinate on the face of the detector. $E(\omega)$ is required for dimensional reasons and is a slowly varying function that can be taken to be constant in the experiments discussed in this paper. Finally, $g\left(\mathbf{r},\omega,\mathbf{p}\right)$ is the optical transfer function or Green's function determined by the classical linear optical system between the source and the detector. It may be worth noting that classically this quantity connects electromagnetic fields that live in real space-time while in the quantum mechanical context it is a mapping of operators that operate in Fock space. This dual nature is the source of many results in this paper and is also the source of confusion about the "photon". It is important to recognize that linear superposition in classical electromagnetic theory plays an essential role in determining g. In the quantum mechanical case g is best thought of as being determined by the boundary conditions defining the modes of the system independently of the state of the system. That is, the modes are the same whether the system is in a one photon state or in a "classical" state for which modes are excited by coherent states.

As an example of the computation of g, we consider arm A of fig. 1. We use the notation $t(\mathbf{x})$ for the transfer function of the object where $\mathbf{x}$ is the transverse spatial vector in the plane of T. The thin lens transformation is

$$l(\mathbf{x},f) = \psi(|\mathbf{x}|, -\frac{\omega}{c}\frac{1}{f}) \tag{45}$$

where f is the focal length and $\mathbf{x}$ is the transverse coordinate in the plane of the lens. Then, after integrating over the plane of D1,

$$\begin{aligned} g_A\left(\mathbf{r}_1,\omega,\mathbf{p}\right) = & \int d^2x_a \int d^2x_f \int d^2x_s t(\mathbf{x}_a) h_\omega(\mathbf{x}_a - \mathbf{x}_f, d_1') \times \\ & l(\mathbf{x}_f,f) h_\omega(\mathbf{x}_f - \mathbf{x}_s, d_1) e^{i\mathbf{p}\cdot\mathbf{x}_s}. \end{aligned} \tag{46}$$

where $\mathbf{r}_1 = (d_1 + d_1')\widehat{\mathbf{e}}_z$, $\mathbf{x}_s$ is in the output plane of the source, and in the Fresnel approximation

$$h_\omega(\mathbf{x},d)=\left(\frac{-i\omega}{2\pi c}\right)\frac{e^{i(\omega/c)d}}{d}\psi(|\mathbf{x}|,\frac{\omega}{c}\frac{1}{d}) \tag{47}$$

$$\psi(x,\frac{\omega}{c}P)=e^{i\frac{1}{2}(\frac{\omega}{c})Px^2}. \tag{48}$$

This notation is very convenient [25,28]. Evaluating g_A gives

$$\begin{aligned} g_A\left(\mathbf{r}_1,\omega,\mathbf{p}\right) &= \left(-i2\pi\frac{\omega}{c}\right)\frac{f}{f-d_1'}e^{i\frac{\omega}{c}(d_1+d_1')}\psi(\mathbf{p},-\frac{c}{\omega}D)\times \\ &\int d^2x_a t(\mathbf{x}_a)e^{i\mathbf{p}\cdot\mathbf{x}_a f/(f-d_1')}\psi(\mathbf{x}_a,-k\frac{1}{f-d_1'}), \end{aligned} \tag{49}$$

where $D=d_1+\frac{d_1'f}{f-d_1'}$.

For arm B taking $\mathbf{r}_2=\mathbf{x}+d_2\widehat{\mathbf{e}}_z$ and performing the integration over $\mathbf{x}_s$ assuming that source has a very large cross-section, we have for each plane wave input mode

$$g_B(\mathbf{r}_2,\omega,\mathbf{p})=\int d^2x_s h_\omega(\mathbf{x}-\mathbf{x}_s,d_2)e^{i\mathbf{p}\cdot\mathbf{x}_s}=e^{i(\omega/c)d_2}e^{i\mathbf{p}\cdot\mathbf{x}}\psi(|\mathbf{p}|,-\frac{c}{\omega}d_2) \tag{50}$$

which is the Fresnel approximation to the plane wave $\exp(i\sqrt{(\frac{\omega}{c})^2-\mathbf{p}^2}d_2+\mathbf{p}\cdot\mathbf{x})$. Now consider what happens if we introduce an aperture function in this expression.

B. Ghost interference

Figure 3 shows a schematic of the ghost interference experiment [3]. In this case

$$\begin{aligned} g_A\left((d_1+d_1')\widehat{\mathbf{e}}_z,\omega\right) &= \int d^2x_a\int d^2x_s h_\omega(-\mathbf{x}_a,d_1')t(\mathbf{x}_a)h_\omega(\mathbf{x}_a-\mathbf{x}_s,d_1)e^{i\mathbf{p}\cdot\mathbf{x}_s}. \\ &= \left(\frac{-i\omega}{2\pi c}\right)\frac{e^{i(\omega/c)(d_1'+d_1)}}{d_1'}\int d^2x_a\psi(|\mathbf{x}_a|,\frac{\omega}{c}\frac{1}{d_1'})t(\mathbf{x}_a)e^{i\mathbf{p}\cdot\mathbf{x}_a}\psi(|\mathbf{p}|,-\frac{c}{\omega}d_1) \end{aligned} \tag{51}$$

and

$$g_B\left(d_2\widehat{\mathbf{e}}_z,\omega',\mathbf{p}'\right)=e^{i(\omega'/c)d_2}e^{i\mathbf{p}'\cdot\mathbf{x}_2}\psi(|\mathbf{p}'|,-\frac{c}{\omega}d_2). \tag{52}$$

In the degenerate case, $\omega=\omega'$ may be replaced by $\omega_p/2$ in the ψ-function and $\mathbf{p}'=-\mathbf{p}$. Then defining the biphoton wave function to be

$$\Psi=\int d^2p\int d\nu u(\nu)a_s^\dagger\left(\frac{\omega_p}{2}+\nu,\mathbf{p}\right)a_i^\dagger\left(\frac{\omega_p}{2}-\nu,-\mathbf{p}\right)|0\rangle, \tag{53}$$

the amplitude is given by

$$A_{12}=\frac{e^{-i\omega_p(\tau_1+\tau_2)}/2}{d_1'}\int d\nu u(\nu)e^{i\nu(\tau_1-\tau_2)}A \tag{54}$$

$$\begin{aligned} A &= A_0\int d^2x_a\psi(|\mathbf{x}_a|,\frac{\omega_p}{2c}\frac{1}{d_1'})t(\mathbf{x}_a)\psi(|\mathbf{x}_a-\mathbf{x}_2|,\frac{\omega_p}{2c}\frac{1}{d_1+d_2}) \\ &= A_0\int d^2x_a\psi(x_a,\frac{\omega_p}{2c}\left(\frac{1}{d_1+d_2}+\frac{1}{d_1'}\right))t(\mathbf{x}_a)e^{-i(\omega_p/2c)(\mathbf{x}_2/d_1+d_2)\cdot\mathbf{x}_a}\psi(|\mathbf{x}_2|,\frac{\omega_p}{2c}\frac{1}{d_1+d_2}). \end{aligned} \tag{55}$$

In the far field Fraunhofer approximation we may replace the $\psi's$ in the last line by 1

$$A_{12}=A_0\widetilde{t}(\frac{\omega_p}{2c}\frac{\mathbf{x}_2}{d_1+d_2}) \tag{56}$$

where $\widetilde{t}(\mathbf{p})$ is the Fourier transform of the aperture transfer function.

In the classical source case we take arm A to be the same as in fig. 3. Then from eq. (51) we have

$$|g_A\left((d_1+d_1')\widehat{\mathbf{e}}_z,\omega,\mathbf{p}\right)|^2 = G_A|\int d^2x_a\psi(|\mathbf{x}_a|,\frac{\omega}{c}\frac{1}{d_1'})t(\mathbf{x}_a)e^{i\mathbf{p}\cdot\mathbf{x}_a}|^2 \tag{57}$$

In arm B of the experiment we use the set up shown in fig. 2,

$$g_B(\mathbf{r}_2,\omega,\mathbf{p}) = \int\int d^2x_l d^2x_s h_\omega(\mathbf{x}_2-\mathbf{x}_l,f_2)P(\mathbf{x}_l)l(\mathbf{x}_l,f_2)h_\omega(\mathbf{x}_l-\mathbf{x}_s,d_2)e^{i\mathbf{p}\cdot\mathbf{x}_s} \tag{58}$$

where we have include a finite aperture for the lens, $P(x_l)$. To make the evaluation of the integral simple, we shall take

$$P(\mathbf{x}_l) = e^{-|\mathbf{x}_l|^2/2A}. \tag{59}$$

Then

$$|g_B(\mathbf{r}_2,\omega,\mathbf{p})|^2 = \left(\frac{\omega}{c}\frac{1}{f_2}\right)A^2e^{-(\mathbf{p}-\frac{\omega}{c}\frac{1}{f_2}\mathbf{x}_2)^2A}. \tag{60}$$

In the limit of large A, the exponential will be very small unless $(\mathbf{p}-\frac{\omega}{c}\frac{1}{f_2}\mathbf{x}_2)^2 << 1/A$. In this case we may write to a good approximation

$$|g_B(\mathbf{r}_2,\omega,\mathbf{p}')|^2 = \left(\frac{\omega}{c}\frac{1}{f_2}\right)A\pi\delta^2(\mathbf{p}'-\frac{\omega}{c}\frac{1}{f_2}\mathbf{x}_2). \tag{61}$$

Combining this result with eq. (57) in the far field limit, $d_1'\to\infty$ in the integral, and the classical correlation function eq. (43) gives for eq. (40)

$$C = C_0|\widetilde{t}(\varepsilon\frac{\omega_p}{2c}\frac{\mathbf{x}_2}{f_2})|^2 \tag{62}$$

where the lens L1 in fig. 2 is not necessary.

C. Klyshko picture

Consider an experiment like that shown in fig. 1. For a biphoton source the amplitude for the process can be written as

$$A = \int d^2p g_A(\mathbf{r}_1,\omega,\mathbf{p})g_B(\mathbf{r}_2,\omega,-\mathbf{p}). \tag{63}$$

The Klyshko picture is based on the observation that $g_B(\mathbf{r}_2,\omega,-\mathbf{p}) = g_B(\mathbf{r}_2,-\omega,\mathbf{p})^*$, see for example eq. (52). The complex conjugate Green's function can be viewed as a source located at $\mathbf{r}_2$ progagating backwards in time reaching the SPDC crystal with transverse momentum $\mathbf{p}$. At the crystal the beam propagates forward in time to $\mathbf{r}_1$.

To generalize this picture, suppose that the beams with transverse momentum $\mathbf{p}$ have independent arbitrary phases so eq. (63) now takes the form

$$A = \int d^2p g_A(\mathbf{r}_1,\omega,\mathbf{p})\mathbf{e}^{i\theta_A(\mathbf{p})}g_B(\mathbf{r}_2,\omega,-\mathbf{p})\mathbf{e}^{\mathbf{i}\theta_\mathbf{B}(-\mathbf{p})}, \tag{64}$$

where

$$\begin{aligned}\langle\mathbf{e}^{i\theta_C(\mathbf{p})}\rangle = 0 \quad \langle\mathbf{e}^{i\theta_C(\mathbf{p})}\mathbf{e}^{-i\theta_C(\mathbf{p}')}\rangle = K\delta^{(2)}(\mathbf{p}-\mathbf{p}') \quad C = A \text{ or } B\\ \langle\mathbf{e}^{i\theta_A(\mathbf{p})}\mathbf{e}^{-i\theta_B(\mathbf{p}')}\rangle = 0\end{aligned} \tag{65}$$

and K is a constant. With these assumptions

$$\langle|A|^2\rangle = K\int d^2p|g_A(\mathbf{r}_1,\omega,\mathbf{p})|^2|g_B(\mathbf{r}_2,\omega,-\mathbf{p})|^2 \tag{66}$$

which is of the form of eq. (40) for the classical correlation $q(\mathbf{p},\mathbf{p}') = K\delta^{(2)}(\mathbf{p}'+\mathbf{p})$.

[1] R. S. Bennink, S. J. Bentley, and R. W. Boyd, Phys. Rev. Lett. **89**, 113601-1 (2002).
[2] A. F. Abouraddy, B. E. A. Saleh, A. V. Sergienko, and M. C. Teich, Phys. Rev. Lett. **87**, 123602-1 (2001).
[3] D. V. Strekalov, A. V. Sergienko, D. N. Klyshko, Y. H. Shih, Phys. Rev. Lett. **74**, 3600 (1995).
[4] Y. H. Shih, J. of Mod. Opt. **49**,2275 (2002),
[5] L. A. Lugiato, A. Gatti, and E. Brambilla, J. Opt. B: Quantum Semiclass. Opt. **4**, S176 (2002) and quant-ph/0203046.
[6] A. V. Belinskii and D. N. Klyshko, Laser Phys. **2**, 112 (1992), A. V. Belinskii and D. N. Klyshko, Phys. Uspenkhi **36**, 653 (1993).
[7] T. B. Pittman, Y. H. Shih, D. V. Strekalov, and A. V. Sergienko, Phys. Rev. A **52**, R3429 (1995).
[8] J. Bell, *Speakable and Unspeakable in Quantum Mechanics* , (Cambridge Univ. Press, London and New York, 1993).
[9] D. N. Klyshko, *Photon and Non-linear Optics* (Gordon and Breach Science, New York, 1988).
[10] T. B. Pittman, D. V. Strekalov, D. N. Klyshko, M. H. Rubin, A. V. Sergienko, and Y. H. Shih, Phys. Rev. A **53**, 2804 (1996).
[11] M. D'Angelo and Y. H. Shih, quant-ph/0302146.
[12] Recall that a set of objects S is said to be convex if for every pair of points $a, b \in S$ and any $t \in (0,1)$ the points $ta+(1-t)b$ are also in the set. That is to say, the straight line connecting any two point in the set lies in the set.
[13] The completely random state has the property that probability of projecting on to an arbitrary state is independent of the state. In the case in the text, $tr\left(\rho D_0\right) = 1/N$ for any state ρ.
[14] A. Sanpera, R. Tarrach and G. Vidal, Phys. Rev. A **58**, 826 (1998), K. Zyczkowski, *et. al.*, Phys. Rev. A **58**, 883 (1998), A. Pittenger and M. H. Rubin, Phys. Rev. A **62**, 032313 (2000).
[15] K. Kraus, *States, Effects, and Operations, (* Springer-Verlag, Berlin, 1983).
[16] A. Peres, *Quantum Theory:Concepts and Methods*, (Kluwer Academic Publishers, Dordrecht, 1993).
[17] N. Gisin, Helv. Phys. Acta **62**, 363 (1989), L. P. Hughston, R. Jozsa, and W. K. Wooters, Phys. Lett. A **183**, 14 (1993).
[18] M. H. Rubin, Phys. Rev. A **61**, 022311 (2000).
[19] T. Aichele, A. I. Lvovsky, and S. Schiller, European Physical Journal D 18, 237 (2002).
[20] M. Horodecki, P. Horodecki, and R. Horodecki, Phys. Lett. A **223**, 1 (1996).
[21] B. M. Terhal, Phys. Lett. A **271**, 319 (2000).
[22] A. Pittenger and M. H. Rubin, Lin. Alg. Appl. **346** , 75 (2002).
[23] O. Gühne, P. Hyllus, D. Bruss, A Ekert, M. Lewenstein,C. Macchiavello, A. Sanpera, Phys. Rev. A **66**, 062305 (2002) and quant-ph/0205089.
[24] A. O. Pittenger and M. H. Rubin, Phys. Rev. A **67**, 012327 (2003).
[25] M. H. Rubin, Phys. Rev. A **54**, 5349 (1996).
[26] J. W. Goodman, *Introduction to Fourier Optics*, (McGraw-Hill Publishing Co.,New York, 1968).
[27] A. Gatti, E. Brambilla, and L. A. Lugiato, Phys. Rev. Lett. **90**, 133603 (2003) and quant-ph/0210109,
[28] A. VanderLugt, *Optical Signal Processing*, (John Wiley& Sons, Inc., 1992). We use slightly different notation than that used in this text.
[29] S. Popescu, Phys. Rev. Lett. **74**, 2619 (1995).

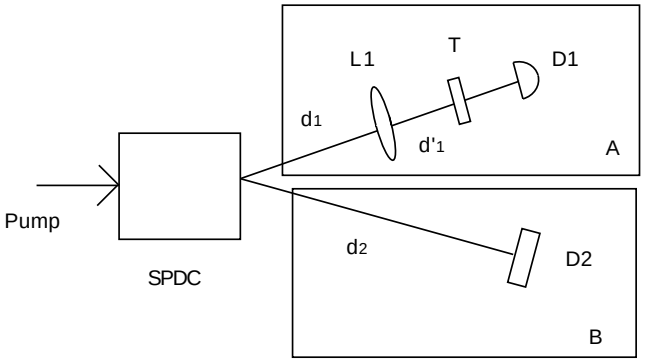

FIG. 1. Illustration of an SPDC experiment. In arm A there is a lens L1 a distance d_1 from the output face of the SPDC crystal and an aperture T a distance d_1' behind it. A fixed detector D1 that collects all the light that is transmitted through T. In arm B the D2 is a planar array of detectors located a distance d_2 from the crystal. The coincidence circuit has been omited.

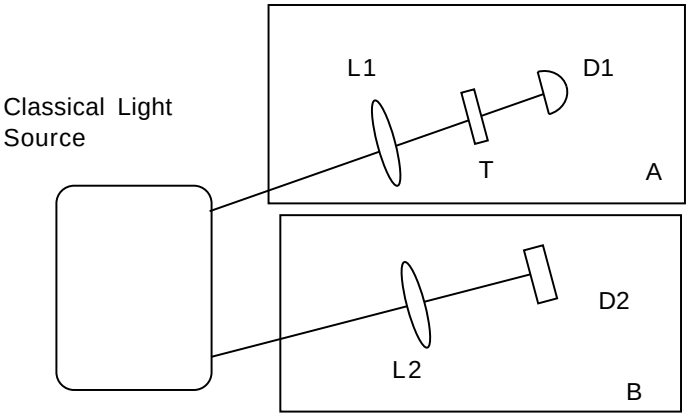

FIG. 2. Illustration of a classical analog of the experiment in fig.1. The detectors are the same as those in fig. 1. The source is understood to be a stocastic source that emits pairs of identical pulses into A and B. The transverse wave number varies randomly from pulse pair to pulse pair. The lenses can be thought of as part of the source or as part of the optical systems in the two arms. However, it is important that T lies in the focal plane of the lens L1 and the detector array plane lies in the focal plane of L2.

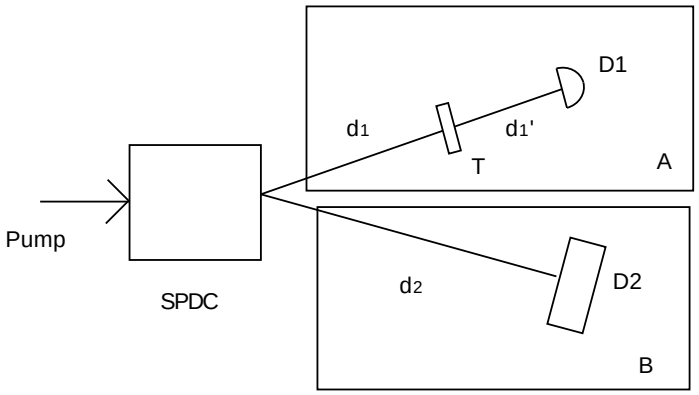

FIG. 3. Illustration of the ghost interference experiment. The aperture T is a double slit and the detector D1 is in the far field and only collects light with zero transverse wave number.